



ELSEVIER

Available online at www.sciencedirect.com

SCIENCE @ DIRECT®

International Communications in
**HEAT and MASS
TRANSFER**

International Communications in Heat and Mass Transfer 32 (2005) 1289–1297

www.elsevier.com/locate/ichmt

Laminar natural convection in cavities filled with circular and square rods[☆]

Edimilson J. Braga, Marcelo J.S. de Lemos^{*}

Departamento de Energia, IEME, Instituto Tecnológico de Aeronáutica, ITA, 12228-900-São José dos Campos, SP, Brazil

Available online 26 August 2005

Abstract

This work compares heat transfer characteristics across a square cavity partially filled with a fixed amount of conducting solid material. The solid phase is shaped into two different geometries, namely square and cylindrical rods, which are horizontally displaced inside the cavity. Comparisons are obtained by numerically solving a conjugate heat transfer problem that considers both the solid and the fluid space. Governing equations are solved using the finite volume method and the algebraic equation set is relaxed with the SIP procedure. The average Nusselt number at the hot wall, obtained from the cavity with square obstacles and for several Darcy numbers, are compared with those calculated with circular obstacles. When comparing the two geometries considering the same modified Rayleigh number Ra_m , this study shows that the average Nusselt number for cylindrical rods are slightly lower than those for square rods.

© 2005 Elsevier Ltd. All rights reserved.

Keywords: Natural convection; Conjugated heat transfer; Circular rods; Square rods; Porous cavity

1. Introduction

Natural convection in fluid saturated enclosures having a distributed solid phase constitutes an important configuration with several applications in engineering, science and environmental analyses. Heat exchangers, underground spread of pollutants, environmental control, grain storage, food

[☆] Communicated by J.P. Hartnett and W.J. Minkowycz.

^{*} Corresponding author.

E-mail address: delemos@mec.ita.br (M.J.S. de Lemos).

processing, packed-bed catalytic reactors and nuclear reactor safety are just some applications of this subject of study. In some cases, such systems can be treated as a porous medium, which can be investigated by suitable mathematical analyses.

Accordingly, models found in the literature dealing with flows in porous media are mostly based on experimental and averaging procedures. The well known *macroscopic* approach, based on the volume average principles, is traditionally used in the analysis of flows in several media such as soil and packed beds. However, this approach gives no details at the pore level. On the other hand, porous media problems can be tackled by means of the *microscopic* approach, which solves the Navier–Stokes equation at the particle level, although the computational cost involved is considerably higher. The understanding of the properties of such *microscopic* approach can, ultimately, aid the development of less expensive *macroscopic* models when dealing with natural convection in porous media.

Studies considering the distribution of a fixed amount of solid material inside an enclosure for laminar buoyancy driven flows can be found in House et al. [1] for the case of a single conducting square solid located at the center of a square cavity. The work of Merrikh and Mohamad [2] also considered heat transfer from within a fluid saturated enclosure with thermal energy being generated by discrete, disconnected solid bodies. Later, in Merrikh et al. [3], a study in which the *continuum* and the *porous-continuum* models were compared for natural laminar convection in a non-homogeneous differentially heated enclosure, without heat generation, was documented. A work also considering the laminar macroscopic and microscopic approach for circular cylinders is presented in Massarotti et al. [4]. In the work of Merrikh et al. [5] an extension of the work performed by Merrikh and Mohamad [2] was carried out. Finally, in Merrikh and Lage [6,7], the effects of distributing a fixed amount of solid material inside a porous medium enclosure on the heat transfer process were recently studied.

Motivated by the foregoing, both laminar and turbulent buoyant flows in porous media considering the macroscopic approach were documented in de Lemos and Braga [8,9] and comparisons between microscopic and macroscopic computations for natural convection were carried out in Braga and de Lemos [10]. All of these papers are part of a systematic development of a turbulence model for flow in porous media based on the *double-decomposition* concept [11–15], which has been also applied to non-buoyant heat transfer [16,17], mass transfer [18], double-diffusion [19], thermal non-equilibrium transport [20], interface problems [21–23] and flow in pipes with porous inserts [24].

Following this systematic analysis, this work presents numerical solutions for steady laminar natural convection within a square cavity filled with a fixed amount of conducting solid material consisting of either circular or square obstacles. Laminar flow is here considered first with turbulence to be added in the future. The long-term objective of this contribution is to compare overall heat transfer characteristics across filled cavities when the solid phase presents different morphologies.

2. Problem considered

The problem here investigated is schematically presented in Fig. 1, which considers a square cavity of side $H=1\text{ m}$ partially filled with a fixed amount of conducting solid material in the form of circular obstacles of diameter D_p (Fig. 1a) and with square rods of size D_p (Fig. 1c). In both cases, the size of the rods is such that the amount of solid material is the same. Corresponding computational grids are shown in Fig. 1b and d, respectively. The rods are equally distributed within the cavity. Also, the enclosure is isothermally heated from the left, with temperature T_H prevailing over that side, and cooled from the

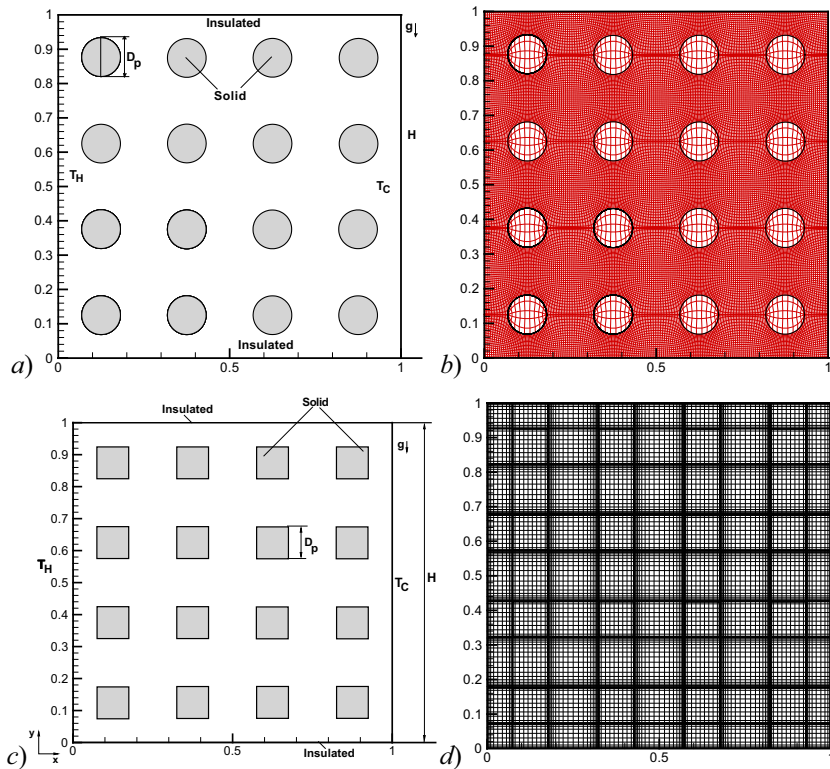


Fig. 1. Schematic of the problem. Cavity with: a) circular rods and b) elliptically generated grid; c) square rods; and d) algebraically generated grid.

opposing surface, where a constant temperature T_C is maintained. The horizontal walls are kept insulated. To analyze such an arrangement, the *microscopic* approach is here employed, in which the flow equations are solved within the void (fluid) space. Results for the case of square rods (Fig. 1c–d) were fully documented in Braga and de Lemos [10] and for that they will just be reproduced here for the sake of comparison and clarity.

3. Governing equations and numerics

For steady flow, the equations for continuity, momentum and temperature take the form:

$$\frac{\partial u}{\partial x} + \frac{\partial v}{\partial y} = 0 \tag{1}$$

$$u \frac{\partial u}{\partial x} + v \frac{\partial u}{\partial y} = -\frac{1}{\rho} \frac{\partial P}{\partial x} + \nu \nabla^2 u \tag{2}$$

$$u \frac{\partial v}{\partial x} + v \frac{\partial v}{\partial y} = -\frac{1}{\rho} \frac{\partial P}{\partial y} + \nu \nabla^2 v + g\beta(T - T_{ref}) \tag{3}$$

$$u \frac{\partial T}{\partial x} + v \frac{\partial T}{\partial y} = \alpha \nabla^2 T \quad (4)$$

where u and v are the velocity components in x and y directions respectively, ρ is the density of the fluid, P is the total pressure and ν is the kinematic viscosity of the fluid. The gravity acceleration is defined by g and β is the thermal expansion coefficient. T and T_{ref} are the temperature and the reference temperature, respectively, and α is the thermal diffusivity.

The rods inside the cavity participate on the momentum transfer through their fluid–solid interfaces, over which, in turn, the no-slip condition was applied. The blocks are conducting and the energy balance equation valid inside them is given by:

$$k_s \nabla^2 T = 0. \quad (5)$$

The numerical method employed for discretizing the governing equations is the control-volume approach with a collocated grid. Further, the grids shown in Fig. 1 were elliptically generated for the circular rod case (Fig. 1a) and algebraically calculated for the square obstacles (Fig. 1c). A hybrid scheme, upwind differencing scheme (UDS) and central differencing scheme (CDS), was used for interpolating the convection fluxes. The well-established SIMPLE method [25] was followed for handling the pressure–velocity coupling. The algebraic equation system was relaxed by the SIP procedure [26].

4. Non-dimensional parameters

For analyzing the configurations of Fig. 1, one can define a modified Rayleigh number Ra_m in the form,

$$Ra_m = Ra_f Da_{\text{eq}} \quad (6)$$

with,

$$Ra_f = \frac{g\beta H^3 (T_H - T_C)}{\nu\alpha} \quad (7)$$

$$Da_{\text{eq}} = \frac{K_{\text{eq}}}{H^2} \quad (8)$$

where Da_{eq} and K_{eq} are “equivalent” permeability and Darcy number, respectively, for the configurations of Fig. 1.

If values for Ra_f and Da_{eq} are selected such that Ra_m is kept constant, a family of cases is obtained. Each case might represent distinct systems consisting of different fluids and solid distribution, but all having the same modified Rayleigh number Ra_m . Considering such premise, the present work intends to study a family of cases with different fluids in distinct media, having all of them $Ra_m = 10^4$.

In order to associate an equivalent value for the permeability of the arrangements in Fig. 1a and c, the correlation of Nakayama and Kuwahara [27] is applied. That correlation is based on the work of Ergun [28] and reads,

$$K_{\text{eq}} = \frac{D_p^2 \phi^3}{c(1-\phi)^2}; \begin{cases} c = 144 \text{ for circular rods} \\ c = 120 \text{ for square rods} \end{cases} \quad (9)$$

where D_p , as seen, is a characteristic dimension of the rod and $\phi = \Delta V_f / \Delta V$. For the geometries of Fig. 1, the porosity ϕ calculated as,

$$\phi = 1 - N \frac{\pi}{4} (D_p/H)^2 \text{ for circular rods} \quad (10)$$

and

$$\phi = 1 - N (D_p/H)^2 \text{ for square rods} \quad (11)$$

is kept constant for a variable number of rods N .

5. Results and discussion

In order to validate the code, a case with a single conducting square solid located at the center of the cavity was run showing good agreement with those summarized in Table 1.

As said, the main idea of this work is to compare heat transfer simulations in a square cavity filled with two types of obstacles, namely, circular and square rods. Comparisons are based on similar conditions in order to verify if the two geometries considered yield equivalent values for the overall Nusselt numbers. For circular rods, runs were performed with grids of sizes 120×120 , 160×160 and 200×200 control volumes for $N=4$, $N=16$ and $N=64$, respectively, where N is the number of obstacles inside the cavity.

For the sake of comparison, all cases were run with $Ra_m = Ra_f Da_{\text{eq}} = 10^4$. A Darcy number was then associated with the flow in the arrangements of Fig. 1 with a permeability K_{eq} calculated by expression (9). If the two geometries here considered have the same porosity $\phi = \Delta V_f / \Delta V$, then the used of (9) yield a permeability K_{eq} for circular rods greater than that calculated for square obstacles. This result, however, is expected since it is easier for a bulk of fluid to flow through a bed with circular rods, which poses less resistance to fluid particles for the same imposed pressure drop.

Further, for an arrangement containing either circular or square rods, distinct values of the D_p yielded different K_{eq} values. However, from the definitions of Ra_f and Da_{eq} , for different Darcy numbers one has to modify the value of Ra_f in order to keep Ra_m fixed at 10^4 . Thus, coefficient β in Eq. (7) is assumed to be the parameter to maintain Ra_m constant when the permeability is varied, since the other quantities are kept fixed. Also, in all cases here analyzed solid obstacles in the cavity yield an overall cavity porosity $\phi=0.84$. The fluid Prandtl number, Pr , and the conductivity ratio between the solid and fluid phases, k_s/k_f , were assumed to be equal to unity.

Figs. 2 and 3 show the streamlines and isotherms, respectively, for a square cavity filled with circular and square obstacles. For circular rods the equivalent Da_{eq} ranged from 0.8188×10^{-2} to 5.1178×10^{-4} whereas for

Table 1

Average Nusselt number for a square cavity with a single conducting solid at the center; $Ra_f=10^5$, $Pr=0.71$ (unless otherwise noted)

Ra_f	D_p [m]	k_s/k_f	House et al. [1]	Merrikh and Lage [6]	Present results $Pr=1$
10^5	0.5	0.2	4.624	4.605	4.667
10^5	0.5	5.0	4.324	4.280	4.375

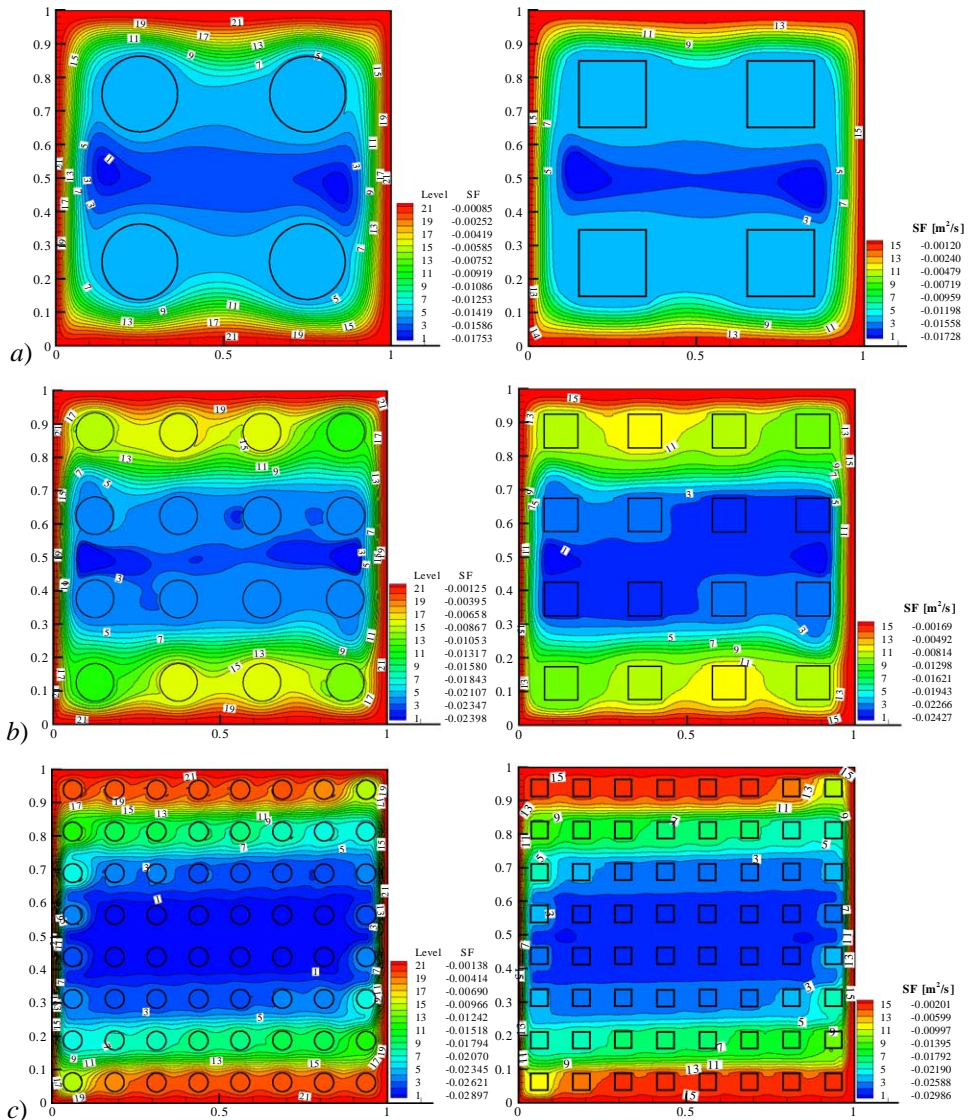


Fig. 2. Streamlines for a square cavity filled with circular (left) and square (right) obstacles with, $Ra_m=10^4$, $\phi=0.84$ and $k_s/k_f=1$; a) $N=4$, b) $N=16$, c) $N=64$.

square obstacles the range for Da_{eq} was 0.7717×10^{-2} to 4.823×10^{-4} . All values for square rods were taken from Braga and de Lemos [10] where a more in dept analyses for that geometry can be found.

Also, according to Braga and de Lemos [10], the higher the number of obstacles inside the clear cavity, the higher the similarity of the flow pattern between the two models, i.e., the *microscopic* and the *macroscopic* approaches resemble each other for greater values of N . In other words, the macroscopic model seems to be more representative of reality when the number of obstacles inside the cavity is higher, which, in turn, correspond to lower permeability cases. However, the lower the permeability, the higher the difference between the average Nusselt numbers between the two models (see [10]).

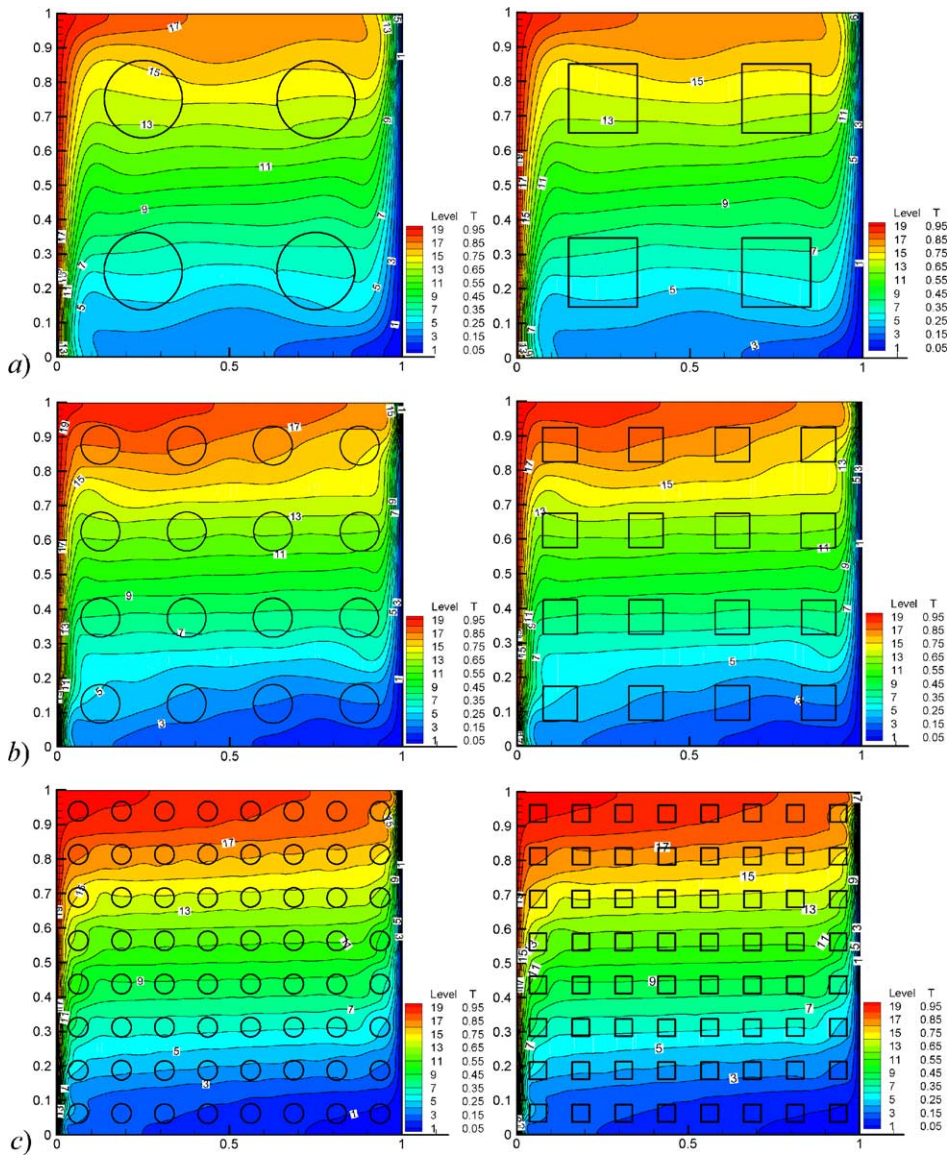


Fig. 3. Isotherms for a square cavity filled with circular (left) and square (right) obstacles with, $Ra_m = 10^4$, $\phi = 0.84$ and $k_s/k_f = 1$; a) $N=4$, b) $N=16$, c) $N=64$.

Fig. 2 clearly shows that the recirculation intensity increases as the medium permeability decreases and the flow patterns comprises primarily cells of relatively high velocity, which circulate around of the entire cavity. However, the secondary recirculation that appears in the center of the cavity, for the higher Darcy numbers analyzed, tends to disappear as the permeability decreases. In a similar way, the temperature gradients are stronger near the vertical walls, but decrease at the center. Fig. 3 also shows that, the higher the number of obstacles, the higher the stratification of the thermal field. According to Merrikh and Lage [6], as the number of square rods increases, and their size becomes reduced, the flow tends to migrate away from the wall towards the center of the cavity. This phenomenon is seen in Merrikh and Lage [6] as a response of the

Table 2

Average Nusselt number for a square cavity filled with obstacles with fixed $Ra_m=10^4$, $\phi=0.84$ and $k_s/k_f=1$

Rod type	$N=1$		$N=4$		$N=16$		$N=64$	
	Da_{eq}	Nu	Da_{eq}	Nu	Da_{eq}	Nu	Da_{eq}	Nu
□	0.3087×10^{-1}	6.5254	0.7717×10^{-2}	9.6204	1.929×10^{-3}	13.7276	4.823×10^{-4}	19.4821
○	0.3249×10^{-1}	6.4315	0.8188×10^{-2}	9.4945	2.047×10^{-3}	13.6534	5.1178×10^{-4}	18.2165

□, Square rods; ○, circular rods.

system due to the increasing flow resistance closer to the solid wall, as the obstacles get closer to the solid surface.

Further, the available literature shows that for the non-Darcy regime in a porous cavity [29–31], fluid flow and heat transfer depend on the fluid Rayleigh number, Ra_f , and on the Darcy number, Da , when other parameters, such as porosity, Prandtl number, and conductivity ratio between the fluid and solid matrix, are held constant. In Braga and de Lemos [9], it was shown that for a fixed Ra_m , the lower the permeability (lower Da), the higher the average Nusselt number at the hot wall. It then looks evident that different combinations of Ra_f and Da yields different heat transfer results, even when Ra_m is the same. The increasing of the fluid Rayleigh number increases natural convection intensity inside the enclosure. For a fixed Ra_m , a higher fluid Rayleigh number is associated with a less permeable media (i.e. lower Darcy number).

Finally, Table 2 compares the behavior of the average Nusselt number for the two geometries investigated, namely, the circular and square shapes. It is clearly seen in Table 2 that the overall values of average Nusselt number, when circular cylinders are considered, are slightly lower than those obtained with the square obstacles. Fluid boundary layers past a square obstacle will separate earlier at the sharp edges than in the case of smoothly varying cylindrical surfaces. Then, larger wakes downstream square obstacles appear. The strength of the recirculatory motion past square obstacles will agitate the fluid with a stronger intensity than in the case of circular rods, where the flow tends to become attached to the solid surfaces. As a result of such a less streamlined flow, heat transfer across the cavity will be higher for the square rod configuration, yielding a higher Nusselt number than those calculated for the circular rod cases.

6. Conclusions

This work compared heat transfer across a square cavity partially filled with a fixed amount of a conducting solid shaped with two different types of geometry. The two geometries herein considered were rods with square and circular forms. The work consisted in numerically solve the momentum and energy equations that resemble a conjugate heat transfer problem in both the solid and the void space. Governing equations are discretized using the finite volume method.

The overall values of the average Nusselt number, when circular cylinders were considered, are slightly lower than those obtained with the square obstacles. A possible explanation for such behavior is that separation of the flow past the edges of square obstacles agitates the flow more intensively, ultimately promoting heat mixing in the cavity. However, for the cases investigated here, this difference is not significant and from an engineering standpoint both shapes play similar roles in the overall heat transfer process.

Future work intends to analyze cavities filled with obstacles of different geometries and quantities in order to study the influence of the medium morphology on the heat transfer process.

Acknowledgments

The authors are thankful to CNPq and FAPESP, Brazil, for their financial support during the course of this research.

References

- [1] J.M. House, C. Beckermann, T.F. Smith, *Numer. Heat Transf.*, A 18 (1990) 213.
- [2] A.A. Merrikh, A.A. Mohamad, J. *Enhanc. Heat Transf.* 8-1 (2001) 55.
- [3] A.A. Merrikh, J.L. Lage, A.A. Mohamad, in: Z. Chen, R. Erwin (Eds.), *Comparison Between Pore-Level and Porous Medium Models for Natural Convection in a Non-Homogeneous Enclosure, Fluid Flow and Transport in Porous Media: Mathematical and Numerical Treatment, Contemporary Mathematics*, vol. 295, 2002, p. 387.
- [4] N. Massarotti, P. Nithiarasu, A. Carotenuto, *Int. J. Numer. Methods Heat Fluid Flow* 13 (7) (2003) 862.
- [5] A.A. Merrikh, J.L. Lage, A.A. Mohamad, *J. Porous Media* 8 (2) (2005) 149.
- [6] A.A. Merrikh, J.L. Lage, Effect of Distributing a Fixed Amount of Solid Constituent inside a Porous Medium Enclosure on the Heat Transfer Process, ICAPM 2004—Proceedings of Intern. Conf. Applications of Porous Media, 2004, p. 51.
- [7] A.A. Merrikh, J.L. Lage, *Int. J. Heat Mass Transfer* 48 (7) (2005) 1361.
- [8] M.J.S. de Lemos, E.J. Braga, *Int. Commun. Heat Mass Transfer* 30 (5) (2003) 615.
- [9] E.J. Braga, M.J.S. de Lemos, *J. Heat Mass Transf.* 47 (26) (2004) 5639.
- [10] Braga, E.J., M.J.S., de Lemos, *Int. J. Heat Mass Transfer* (in press).
- [11] M.H.J. Pedras, M.J.S. de Lemos, *Int. Commun. Heat Mass Transfer* 27 (2) (2000) 211.
- [12] M.H.J. Pedras, M.J.S. de Lemos, *Int. J. Heat Mass Transfer* 44 (6) (2001) 1081.
- [13] M.H.J. Pedras, M.J.S. de Lemos, *Numer. Heat Transf., A Appl.* 39 (1) (2001) 35.
- [14] M.H.J. Pedras, M.J.S. de Lemos, *J. Fluids Eng.* 123 (4) (2001) 941.
- [15] M.J.S. de Lemos, M.H.J. Pedras, *J. Fluids Eng.* 123 (4) (2001) 935.
- [16] F.D. Rocamora Jr., M.J.S. de Lemos, *Int. Commun. Heat Mass Transfer* 27 (6) (2000) 825.
- [17] M.J.S. de Lemos, F.D. Rocamora, Turbulent Transport Modeling for Heated Flow in Rigid Porous Media, Proceedings of the Twelfth International Heat Transfer Conference, Grenoble, France, August 18–23, 2002, p. 791.
- [18] M.J.S. de Lemos, M.S. Mesquita, *Int. Commun. Heat Mass Transfer* 30 (1) (2003) 105.
- [19] M.J.S. de Lemos, L.A. Tofaneli, *Int. J. Heat Mass Transfer* 47 (19–20) (2004) 4221.
- [20] M. Saito, M.J.S. de Lemos, *Int. Commun. Heat Mass Transfer* 32 (5) (2005) 667.
- [21] R.A. Silva, M.J.S. de Lemos, *Numer. Heat Transf., A Appl., USA* 43 (6) (2003) 603.
- [22] R.A. Silva, M.J.S. de Lemos, *Int. J. Heat Mass Transfer* 46 (26) (2003) 5113.
- [23] M.J.S. de Lemos, *Int. Commun. Heat Mass Transfer* 32 (1–2) (2005) 107.
- [24] M. Assato, M.H.J. Pedras, M.J.S. de Lemos, *J. Porous Media* 8 (2005) 13.
- [25] S.V. Patankar, D.B. Spalding, *Int. J. Heat Mass Transfer* 15 (1972) 1787.
- [26] H.L. Stone, *SIAM J. Numer. Anal.* 5 (1968) 530.
- [27] Nakayama, F. Kuwahara, *J. Fluids Eng.* 121 (1999) 427.
- [28] S. Ergun, *Chem. Eng. Prog.* 48 (1952) 89.
- [29] A.A. Merrikh, A.A. Mohamad, *Int. J. Heat Mass Transfer* 45 (2002) 4305.
- [30] J.C. Kalita, D.C. Dalal, A.K. Dass, *Phys. Rev., E* 64-066703 (2001) 1.
- [31] J.L. Lage, A. Bejan, *Numer. Heat Transf., A* 19 (1991) 21.